0038-075C/02/16701-35–48
Soil Science

January 2002
Vol. 167, No. 1
Printed in U.S.A.

NITROGEN OXIDE TRACE GAS TRANSPORT AND TRANSFORMATION: I. EVALUATION OF DATA FROM INTACT SOIL CORES

Rodney T. Venterea[1] and Dennis E. Rolston[2]

Once emitted to the atmosphere, nitric oxide (NO) and nitrous oxide (N_2O) regulate several important processes in the troposphere and stratosphere. Understanding controls over N oxide gas emissions from fertilized soils is often complicated by highly heterogeneous and dynamic field conditions. An intact soil core method is described here for examining multiple subsurface controls concurrently with N oxide surface fluxes under hydrostatic and isothermal conditions dominated by Fickian diffusive transport. The method allows for simultaneous measurement of inorganic N levels, pH, water content, and soil-gas concentrations of NO, N_2O, O_2, and CO_2 and for subsequent calculation of N mass balances, net nitrification rates, CO_2 respiration rates, O_2 uptake rates, fraction of nitrified N lost as gas, and anaerobic microsite fraction profiles. The method is applied to moderately acidic soil fertilized with anhydrous ammonia. Steady nitrification and persistent NO_2^- levels resulted in NO gaseous losses representing 22–37% of the inorganic N initially present and >50% of the nitrified N. Of the initial N mass present, 96–119% was accounted for as N solutes and gases. High N_2O soil-gas concentrations (5–20 mg N m^{-3}) and fluxes (1 mg N m^{-2} h^{-1}) persisted despite anaerobic fractions of ≤ 10^{-10} m^3 anaerobic soil m^{-3} soil, suggesting that N_2O sources other than denitrification were important. (Soil Science 2002;167:35–48)

Key words: Nitrification, denitrification, chemodenitrification, gas diffusion, respiration.

INTEREST in emissions of the nitrogen (N) oxide gases from fertilized agricultural soils has evolved from primarily agronomic concerns (Collison, et al., 1933; Allison, 1955) to more recent recognition of the impact of these gases on a wide range of atmospheric processes, including tropospheric ozone (O_3) regulation, global warming, and atmospheric deposition of N and acidity (Crutzen, 1981; Vitousek and Matson, 1993). Assessments of global sources of N_2O indicate that agricultural activities have been responsible for more than 70% of the increase in atmospheric concentrations occurring since 1850 (Kroeze, et al., 1999). Emissions of N oxide gases from fertilized soils can be influenced by a relatively wide range of microbial, chemical, and physical soil properties and processes (Hutchinson and Davidson, 1993). Several studies have attempted to elucidate controls over gas fluxes by examining inorganic N levels and/or other controlling variables concurrently with gas fluxes (Matson, et al., 1996; Thornton and Valente, 1996; Röver, et al., 1998). Many of these studies are affected by highly dynamic hydrologic, thermal and chemical conditions in the field. These factors, together with high spatial variability of substrate levels and other controls, complicate the development of relationships between controlling mechanisms and resulting gaseous losses.

Contribution from the Department of Land, Air and Water Resources, University of California, Davis, California 95616

[1]Institute of Ecosystem Studies, Box AB, Millbrook, New York 12545. Dr. Venterea is corresponding author. E-mail: venterear@ecostudies.org

[2]Department of Land, Air and Water Resources, One Shields Avenue,University of California, Davis, California, 95616.

Received Feb. 26, 2001; accepted Sept. 14, 2001.

There have also been very few studies to date where N oxide soil-to-atmosphere fluxes have been measured concurrently with measurements of a comprehensive set of controlling variables such as inorganic N levels, soil pH, water content, aerobic status and subsurface N oxide gas concentrations in soil profiles directly beneath the location of flux measurements.

Anhydrous ammonia (AA) is one of the most commonly used N fertilizers in many parts of the world (Stehouwer and Johnson, 1990; Bouman, et al., 1995; Strong and Cooper, 1992; California Department of Food and Agriculture, 1998). Studies have shown that nitrite (NO_2^-) can accumulate to significant levels following AA application (Chalk, et al., 1975). It is also known that elevated NO_2^- levels can, theoretically, promote N oxide gas production caused by abiotic decomposition of nitrous acid (HNO_2) that forms via the protonation of NO_2^- at low pH ($pK_a = 3.3$) (Van Cleemput and Samater, 1996). However, little information is available regarding the potential magnitude of gaseous losses under these conditions relative to the amount of N fertilizer applied or the amount of N passing through the nitrification process. In addition, there have been very few, if any, studies which have been able assess the relative importance of HNO_2-mediated reactions in driving N_2O emissions compared with other processes (e.g., denitrification).

The objective of the present study was to develop and implement an intact soil core method for examining proximal controls over N oxide emissions using soil cores sampled after AA application to a moderately acidic loam soil. The method allows for (i) repeated measurement of inorganic N concentrations, pH, and water content at 25-mm depth intervals, (ii) corresponding measurements of soil-gas concentrations of NO, NO_2, N_2O, O_2 and CO_2 at 20-mm depth intervals, and (iii) corresponding measurements of N oxide fluxes under hydrostatic and isothermal conditions. The data set is used to perform a N mass balance analysis, to calculate nitrification, CO_2 respiration and O_2 uptake rates, and to estimate anaerobic microsite fractions across the depths of each core. The effectiveness of the physical apparatus in minimizing disturbances to gaseous diffusion as the dominant mode of transport is analyzed. In a subsequent paper, the data are used to evaluate reactive transport models and to quantify rates of subsurface gas production and transformation processes (Venterea and Rolston, 2002).

MATERIALS AND METHODS

Sample Collection

Intact soil cores were sampled during the course of a field experiment described previously (Venterea and Rolston, 2000b). Field measurements of NO, N_2O, and CO_2 flux, inorganic N levels, soil pH, water content, and soil temperature were made during July–August 1998 in a furrow-irrigated tomato field in Sacramento County, California. The soil was a moderately acidic loam (thermic Aquic Xerofluvent) of Columbia series (Soil Conservation Service, 1993) comprised of 51% sand, 38% silt, and 11% clay, with 0.9–1.1% organic matter. Within 3 to 7 days following application of 12 g N m^{-2} of AA, six core samples were collected from the 0- to 0.10-m depth at random locations within the AA injection zone. Cores were collected with a manual-driven coring tool containing a 100 mm × 83 mm-ID stainless steel (SS) inner core. Four threaded holes (10 mm diameter) located at 20-mm intervals along the length of each inner core were sealed with rubber discs (2 mm thick) during sampling.

Intact Core Apparatus

Cores were delivered to the laboratory within 1 h and assembled together with the measurement system (Fig. 1). After verifying that NO and N_2O surface fluxes in the six cores were similar (all within the range of 15–25 mg N m^{-2} h^{-1}), three of the cores were randomly selected for further experimentation. The rubber discs were removed and replaced with SS unions, which were machined on the outside end to accept teflon Mininert gas-tight sampling ports with rubber septa and on/off valves (Dynatech, Chantilly, VA). Before attaching the sampling ports, a 40-mm-long needle was installed horizontally through a 1-mm-ID hole in the SS fitting into the center of the soil core. Rigid wire was held inside the needle to prevent clogging during insertion. Each core was fitted on the bottom end with a teflon-lined acrylic cap with a hole in the center to accept a SS union/gas-sample port assembly (with a 5-mm-long needle). The top end of the core was connected to a SS upper chamber (50-mm long × 83-mm ID) via an acrylic union. The upper chamber was fitted on the top with a teflon-lined acrylic cap. Gas-tight seals were achieved by fitting rubber O-rings into 2–3-mm grooves along the perimeter of the acrylic pieces and by clamping the unit together with threaded rods inserted through holes in the union and end caps. The units were maintained at 25 ± 2 °C for the dura-

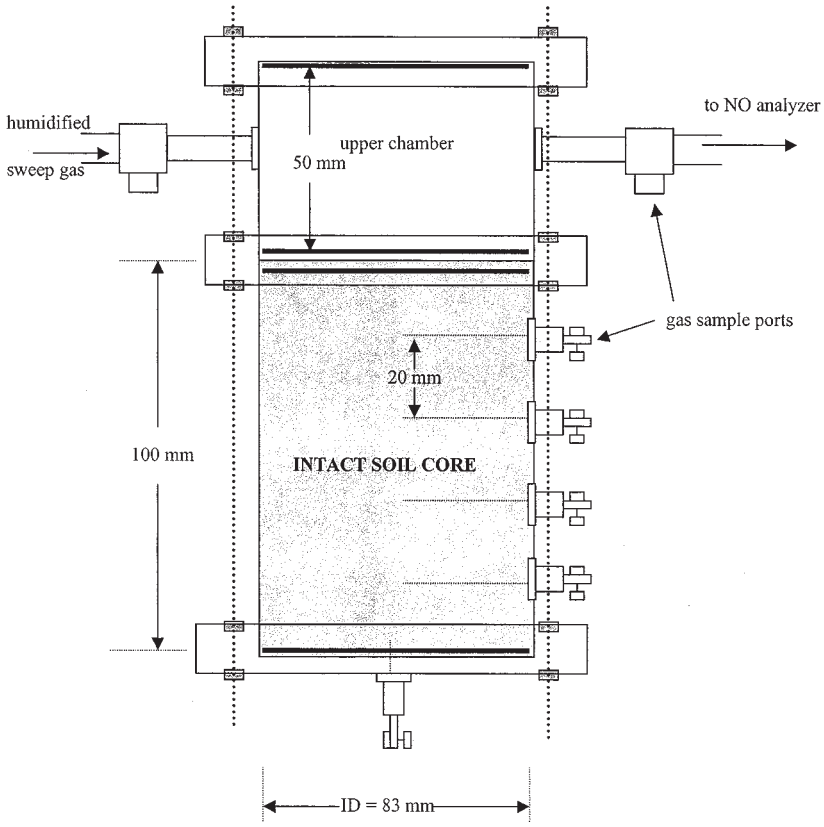

Fig. 1. Intact core apparatus.

tion of the experiment. Two of the three cores (Cores A and B) were maintained at field-collected moisture levels of 0.16–0.21 m^3 H_2O m^{-3} soil, which were representative of mean field moisture conditions measured in the top 0–0.10 m during most of the 50-day field experiment (Venterea and Rolston, 2000b).

Before assembly took place, the third core (Core C) was saturated with 0.01 *M* $CaCl_2$ solution and drained under a constant pressure of 25 kPa for 24 h with a porous ceramic plate in contact with the bottom of the soil, achieving a fairly uniform water content of 0.27 m^3 H_2O m^{-3} soil. The water-amended core was established primarily to provide additional data for subsequent comparison with model predictions (Venterea and Rolston, 2002) and also for further evaluation of the intact core method. Because of lack of replication of the added-water treatment, the Core C data presented here are limited to evaluation of total system N mass balances and the analysis of diffusion processes (described below).

A humidified, carbon-filtered, O_3-free air stream (sweep gas) was delivered through each upper chamber via Teflon tubing (6.35 mm OD) at 0.024–0.036 m^3 h^{-1}. The sweep gas served to maintain trace gas and O_2 concentrations at the soil surface representative of ambient concentrations while minimizing soil drying. Care was taken to ensure that the sweep gas created minimal disturbance to diffusive transport of gases within the soil core and across the soil-atmosphere interface, by verifying that (i) each assembly was leak-tight at pressures $>$ 70 kPa under static conditions, (ii) fluxes of NO and N_2O were independent of the rate of sweep gas flow over the range of 0.01 $-$ 0.06 m^3 h^{-1}, and (iii) measured vertical gas pressure gradients ($<$15 Pa m^{-1}) within the cores were below that which would create significant advective mass flux. Pressure gradients were measured with a transducer needle probe sensitive to 1.5 Pa (Omega PX275–0.1D1) inserted into the side and bottom sampling ports.

Gas Fluxes and Soil-Gas Concentrations

The influent and effluent sweep gas streams were analyzed regularly for NO and nitrogen dioxide (NO_2) concentrations by delivery to a chemiluminescent NO/NO_2 analyzer (model 750B, Sievers) (Venterea and Rolston, 2000a). Stainless steel tee unions fitted with butyl rubber septa were installed in the sweep gas lines for removal of influent and effluent samples using glass/teflon gas tight syringes fitted with on/off valves (Dynatech) for N_2O analysis using gas chromatography (GC) with an electron capture detector (ECD) (Venterea and Rolston, 2000a and b). Periodic sparging of the sweep gases through 0.1 N sulfuric acid and subsequent analysis for dissolved NH_4^+ indicated that emissions of NH_3 gas were unimportant (<0.05 mg N m^{-2} h^{-1}) under these acidic conditions. Fluxes (F_N, mg N m^{-2} h^{-1}) of NO, NO_2, and N_2O were calculated from

$$F_N = \frac{q}{A}(C_e - C_i) \quad (1)$$

where q is the sweep gas flow rate (m^3 h^{-1}), C_e and C_i (mg N m^{-3}) are the effluent and influent gas concentrations, A (m^2) is the area of the soil-atmosphere interface, and N refers to the gas species of interest. The value of A was corrected to account for a decrease in surface area of approximately 7% resulting from each subcore sampling (below). Four times during 1 month (at intervals of 6–14 days) a set of soil-gas samples (500–1000 μL) were taken by syringe from the side and bottom sampling ports. Samples were withdrawn slowly at ~100 μL s^{-1} to minimize internal pressure disturbances. Two syringe samples were taken within a 60-s period and analyzed immediately for NO and NO_2 using the NO/NO_2 analyzer in discrete sample mode. Two additional syringe samples were then taken and analyzed for N_2O by GC/ECD and CO_2 and O_2 using GC with a thermal conductivity detector (Venterea and Rolston, 2000b). Soil-gas NO_2 concentrations were measured on only one occasion for each of the cores. Otherwise, soil-gas sampling was performed immediately before the subcore soil sampling (below).

Soil Subcore Sampling and Analysis

At intervals of 6 to 14 days, the upper chamber was removed from each core and one smaller subcore was taken for determination of mineral N concentrations, soil pH, and water content. The subcores were taken from the center of each quadrant of the core on four separate occasions. An aluminum cylindrical coring tool (120 mm × 19 mm ID × 22 mm OD) was inserted manually to the bottom of the core and removed with soil intact. The resulting hole was immediately filled with a solid teflon rod (100 mm × 22 mm OD). The system was reassembled and the experiment continued. Within 10 min of sampling, soil in the small subcore was extruded and divided into four segments of equal length. Each segment was homogenized manually without sieving and further divided into three portions (the soil contained minimal particles >2 mm in diameter). One portion (~6 g) was immediately extracted with 0.5 *M* K_2SO_4 for analysis of NH_4^+, NO_2^- and NO_3^- (Venterea and Rolston, 2000a). Analysis of NO_2^- was done within 6 h of extraction. Separate portions were taken for pH (~4 g) and water content determination (~2 g) (Venterea and Rolston, 2000a). For purposes of data analysis, it was assumed that values of inorganic N, pH, and water content obtained by this method were representative of conditions averaged over 25-mm layers centered at 12.5-, 37.5-, 62.5-, and 87.5-mm depths. The total mass of soil in each subcore was used to determine bulk density averaged over the 100-mm length. On some occasions, the upper 5 to 10 mm was sampled separately to determine bulk density of soil adjacent to the soil-atmosphere interface.

RESULTS

Solute, pH and Soil-Gas Concentrations

The patterns of N solute and pH dynamics (Fig. 2) indicate steady nitrification, with accumulations of NO_3^- and depletions in NH_4^+ and soil pH continuing for the duration of the experiments. Relatively high variances observed between cores in N solute levels and pH were expected as a result of nonuniformity of anhydrous ammonia application methods (Moraghan, 1980). Levels of NO_2^- were highest during the first 0–17 days and persisted in the range of 10–25 mg N kg^{-1} (higher toward the bottom of the cores) after 25 to 30 days. Previous experiments with this soil and other similar agricultural soils have shown that NO_2^- accumulating under bulk aerobic conditions originates primarily from autotrophic nitrification (Venterea and Rolston, 2000a and b). Soil-gas NO and N_2O levels were in the range of 25 to 100 and 5 to 20 mg N m^{-3}, respectively (Fig. 3). Upon deconstruction of the cores, the bottom (0.10 m) gas sampling port needle in Core B was found to be clogged, so these data were dis-

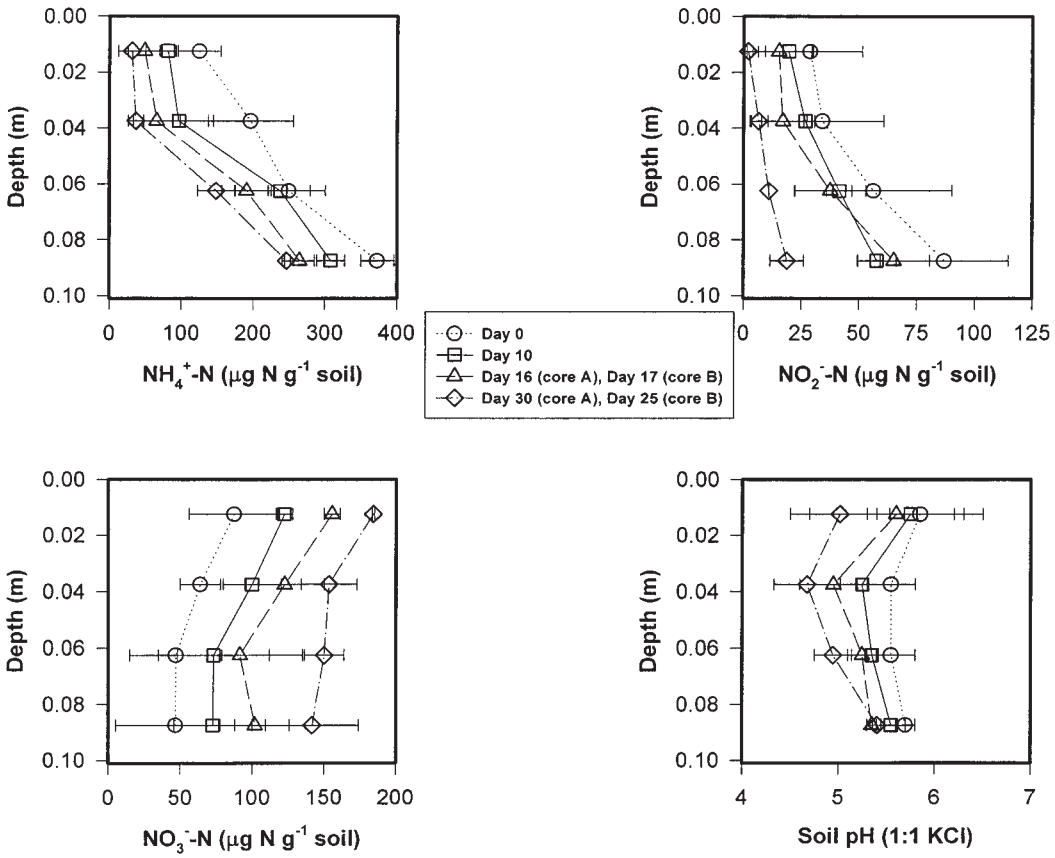

Fig. 2. Depth profiles of N solute concentrations and soil pH within intact soil cores (errors bars = standard error, $n = 2$).

carded. Soil-gas NO_2 concentrations were below detection in all cases (<2 mg N m^{-3}). Nonlinear regression analysis (Sigma Plot, Jandel Scientific) was used to generate estimates of each N solute and gas species as a continuous function of depth. Second- or third-order polynomial functions fit the observed data well (r^2 generally ≥0.95). The total mass (MS_N (t), mg N m^{-2}) of solute species N in the core at sampling time t was then estimated from

$$MS_N(t) = \rho \int_0^L [N_t(z)]dz \qquad (2)$$

where [N_t (z)] is the polynomial expression for soil concentration (mg N kg^{-1} soil) as a function of soil depth (z), L is the core length (0.10 m), and ρ is the dry soil bulk density (kg m^{-3}). Integrals were evaluated analytically using the obtained polynomial functions. The mass of N existing within the core as NO and N_2O, including that in gaseous form and in dissolved form assuming Henry's law partitioning, was estimated to be a small fraction (<0.01%) of the total mass of N present in the core at any time. Therefore, the masses of NO and N_2O within the core were not considered in the total mass balance analysis. Polynomial expressions were also obtained for soil pH. These were used together with NO_2^- concentration profile functions to calculate HNO_2-mediated N oxide production (Venterea and Rolston, 2002).

N Oxide Fluxes

Surface fluxes of NO and N_2O were in the range of 15 to 25 and 1 to 2 mg N m^{-2} h^{-1}, respectively (Fig. 4). Fluxes of NO_2 were not detectable from analysis of the influent and effluent sweep gas (<0.2 mg N m^{-2} h^{-1}). Fluxes of NO showed a pattern of slight increase during the first 6 to 12 days, followed by gradual decline.

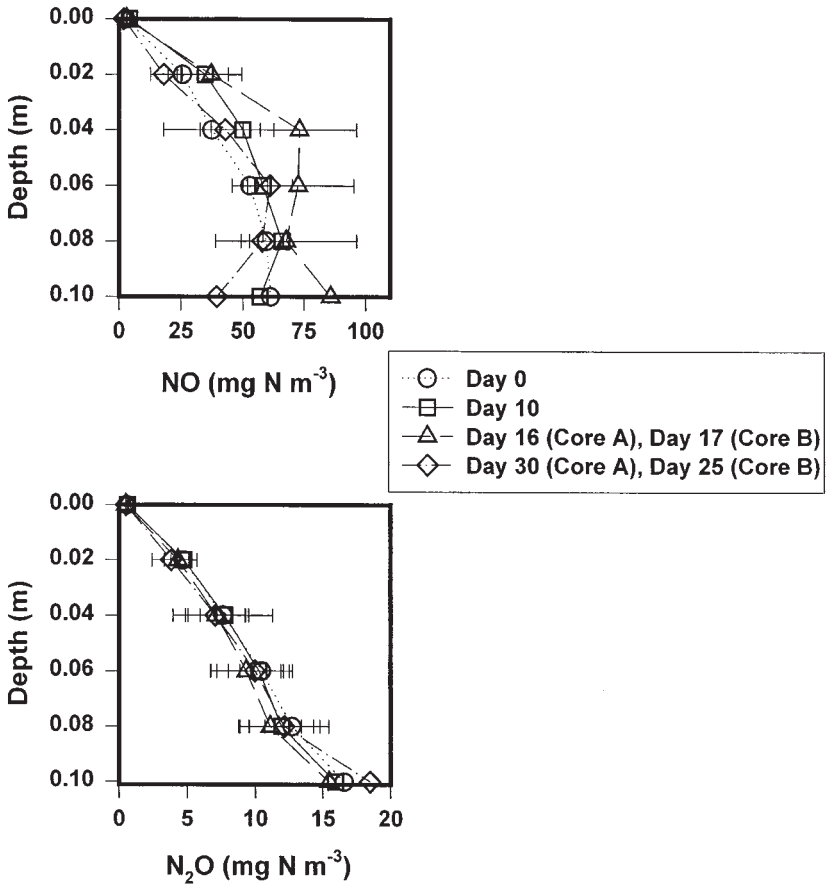

Fig. 3. Depth profiles of NO and N_2O soil-gas concentrations within intact soil cores (errors bars = standard error, $n = 2$).

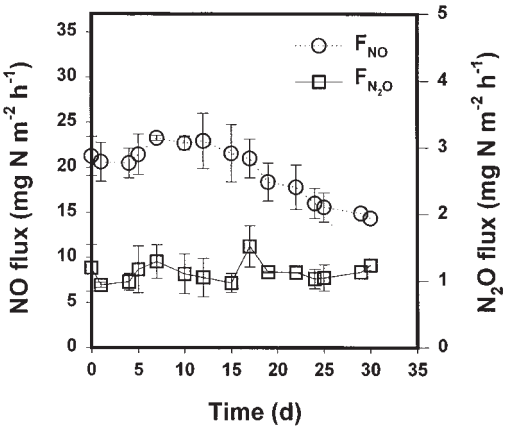

Fig. 4. Fluxes of NO and N_2O from intact soil cores (errors bars = standard error, $n = 2$).

The ratio of NO:N_2O flux at any time varied from 10 to 27. The total mass of NO and N_2O emitted at the soil surface was a significant component of the mass balance, as estimated from

$$MG_N(t_1 \rightarrow t_2) = \int_{t_1}^{t_2} [F_N(t)]dt \qquad (3)$$

where $MG_N(t_1 \rightarrow t_2)$ is the total mass (mg N m^{-2}) of gas species N emitted during time interval t_1 to t_2. These integrals were evaluated numerically using observed F_N versus time data (in Fig. 4) in order to compute the gaseous flux components of the mass balance (Table 1) and the percentages emitted as gases (Fig. 5).

Mass Balances and Nitrification Rates

A total mass balance was evaluated by comparing N solute mass initially present (NH_4^+ + NO_2^- + NO_3^-) with solute mass remaining at

TABLE 1

Mass balance analysis results

	g N m^{-2}						
	Solute mass present			Mass emitted as gas		Total N	% Recovery
	NH_4^+	NO_2^-	NO_3^-	NO	N_2O		
Initial solute mass present:							
Core A	26.3	10.3	5.0			41.6	
Core B	35.3	3.2	12.5			51.0	
Mean (SE)†	30.8 (4.5)	6.8 (3.6)	8.8 (3.3)			46.4 (4.7)	
Final solute mass present and mass emitted as gases:							
Core A	13.3	1.7	18.4	15.4	0.88	49.7	119%
Core B	17.2	0.8	22.7	11.2	0.61	52.6	103%
Mean (SE)†	15.3 (1.9)	1.3 (0.4)	20.5 (2.2)	13.3 (2.1)	0.74 (0.13)	51.1 (1.4)	111% (8.1)

†SE = standard error (n = 2).

the conclusion plus the total mass of N oxide gases emitted using Eqs. (2) and (3) (Table 1). Initial total N concentrations in the cores were in the range of 42 to 51 g N m^{-2}, consistent with the applied dose of 12 g N m^{-2} concentrated within an AA injection zone of ~15% of the total area of the field (Venterea and Rolston, 2000b). Mass emitted as NO and N_2O into the sweep gas accounted for 22–37% and 1.2–2.1%, respectively, of the mass present in the cores initially as N solutes. The total mass recovered as solutes and emitted as gases accounted for 119% and 103% of the initial solute mass in cores A and B, respectively (Table 1). Recoveries of >100% may have been caused, in part, by N mineralization from soil organic matter, which was not accounted for experimentally. The discrepancies in the mass balance would be fully explained by average NH_4^+ mineralization rates of 0.08 and 0.02 mg N kg^{-1} h^{-1} in Cores A and B, respectively. Similar mineralization rates would, in fact, be expected based on previous measurements made in moderately acidic agricultural silt loam (Curtin, et al., 1998) and sandy loam soils (Venterea and Rolston, 2000a) having organic C contents similar to those of the present soil. Soil organic N contents (Kjeldahl digestion) at the conclusion of the present experiment were 0.09 to 0.10%, with no significant differences between cores or trends with soil depth within each core. Analysis of data from Core C also showed near 100% recovery (96%). Additional sources of deviation from 100% include the assumptions that soil properties within each core were laterally homogeneous, and dinitrogen (N_2) gas losses were negligible. Despite these possible sources of error, recoveries of 96 to 119% suggest that the experimental procedure and data analysis were relatively successful in accounting for the dominant N transformations. Mass balance calculations were also performed without reliance on polynomial regression estimates of concentration versus soil depth, i.e., under the assumption that solute concentrations measured within each 25-mm segment of the subcores represented mean concentrations across each respective depth instead. Results were nearly identical to the polynomial method, with estimated mass balances varying by <3%.

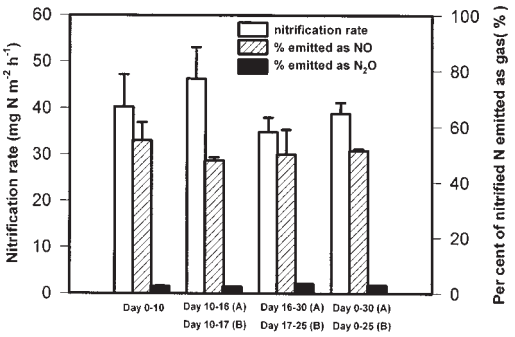

Fig. 5. Nitrification rates estimated using Eq. (4), and percentage of nitrified N emitted as NO and N_2O estimated using Eqs. (3) and (4) (errors bars = standard error, n = 2).

Net nitrification rates for each core were evaluated using the accumulation rate of nitrification product mass, including NO_3^- accumulation within the core and N oxide gases emitted from the core surface during each time interval, according to

$$NR(t_1 \rightarrow t_2) = \frac{[MS_{NO_3^-}(t_2) - MS_{NO_3^-}(t_1)] + [MG_{NO}(t_1 \rightarrow t_2) + MG_{N_2O}(t_1 \rightarrow t_2)]}{t_2 - t_1} \quad (4)$$

where NR ($t_1 \rightarrow t_2$) is the net nitrification rate (g N m^{-2} h^{-1}) during time interval t_1 to t_2, and other terms are defined as in Eqs. (2) and (3). These estimates necessarily represent mean rates during the time interval and across the entire soil depth. Justification for inclusion of both NO and N_2O as nitrification products is based on previous studies (Venterea and Rolston, 2000a) and subsequent analysis presented in this paper and in Venterea and Rolston (2002). Although this analysis suggests that a portion of the N_2O was derived from denitrification, removal of this fraction from the above NR calculations had negligible effects on resulting nitrification rates. The mass balance and nitrification rate results (Fig. 5) indicate that a high fraction of the nitrified N was emitted as N oxide gases at the core surface, with very close agreement between cores. As a percentage of the nitrified N estimated by product accumulation, 52% and 51% was emitted as NO, and 3.0% and 2.8% was emitted as N_2O in Cores A and B, respectively, over the entire duration of the experiments. Nitrification rate calculations performed under the assumption that solute concentrations measured within each 25-mm segment of the subcores represented mean concentrations across each respective depth yielded rates that differed from the polynomial method by <5%.

Diffusion Analysis

The observed gas fluxes were compared with those expected as a result of Fickian diffusion driven by the observed concentration profiles of NO and N_2O. From each set of NO and N_2O soil-gas concentration measurements, gradients in N oxide gas concentration at the soil surface ($z = 0$) were estimated in two ways: (i) by assuming a linear gradient over the upper 20 mm calculated from measured concentrations at the 20-mm depth and in the sweep gas (0 mm), and (ii) using the regression relationships obtained for soil-gas concentrations by taking the analytical derivative of the regression functions at $z = 0$. The expected diffusive flux was then calculated from

$$F_N = -D_{s,N}\left(\frac{dC}{dz}\right)_{z=0} \quad (5)$$

where the term in parentheses is the estimated gradient (mg N m^{-3} gas m^{-1} soil), and $D_{s,N}$ is the effective soil gas diffusion coefficient (m^3 gas m^{-1} soil h^{-1}) of species N. The latter term ($D_{s,N}$) was estimated using the Buckingham-Burdine-Campbell model for gas diffusivity in undisturbed soil (Moldrup, et al., 1999) given by

$$D_{s,N} = D_{o,N}\left(\frac{\epsilon^{2\,+\,3/b}}{\phi^{3/b}}\right) \quad (6)$$

where $D_{o,N}$ is the diffusion coefficient of gas species N in free air (m^2 gas h^{-1}), b is the Campbell soil-water retention parameter (Moldrup, et al., 1996), ϵ is the volumetric air content (m^3 gas m^{-3} soil), and ϕ is the total porosity (m^3 pore volume m^{-3} soil). Values for ϕ were calculated from bulk density measured in the upper 5-mm samples (which was ~10% lower than overall bulk density), and values at $z = 0$ were calculated using regression functions for water content versus depth. Free air diffusivity values (D_o) for NO and N_2O at 25 °C were calculated from the semiempirical Chapman-Enskog model (Bird, et al., 1960). Values of b for this soil were estimated using three different empirical relationships: (i) a soil texture and bulk density function (Moldrup, et al., 1996, Eq. [12]), which yielded $b = 6.2$ for Cores A and B, and 6.0 for Core C, (ii) a soil texture function (Moldrup, et al., 1996, Eq. [11]), which yielded $b = 5.6$, and (iii) a clay fraction function (Rolston and Moldrup, 2002) which yielded $b = 5.0$. These values are consistent with a published b value (5.4 ± 1.9) for loamy texture soils, based on a large set of data ($n = 125$) that was used, in part, to derive empirical relationship (iii) above (Clapp and Hornberger, 1978; Rolston and Moldrup, 2002). Therefore, the sensitivity of predicted fluxes to the estimated b value for the intact soil cores was examined by calculating fluxes using Eqs. (5) and (6) with b values varying by 2.0 of the central estimated value (i.e., 5.6 ± 2.0). Degree of agreement between observed and predicted fluxes was assessed by the root-mean-square error (RMSE) and degree of over- or under-prediction was assessed by the bias (Moldrup, et al., 1997). The results indicate no overall systematic trend of deviation of observed fluxes from that predicted by diffusion (Fig. 6). The linear gradient estimate resulted in RMSE and bias values similar to the nonlinear gradient estimate. Although the RMSE for N_2O flux was somewhat improved at a lower b value (42% and 55% of mean for linear and nonlinear gradient, respectively, at $b = 3.6$), it is clear that sources other

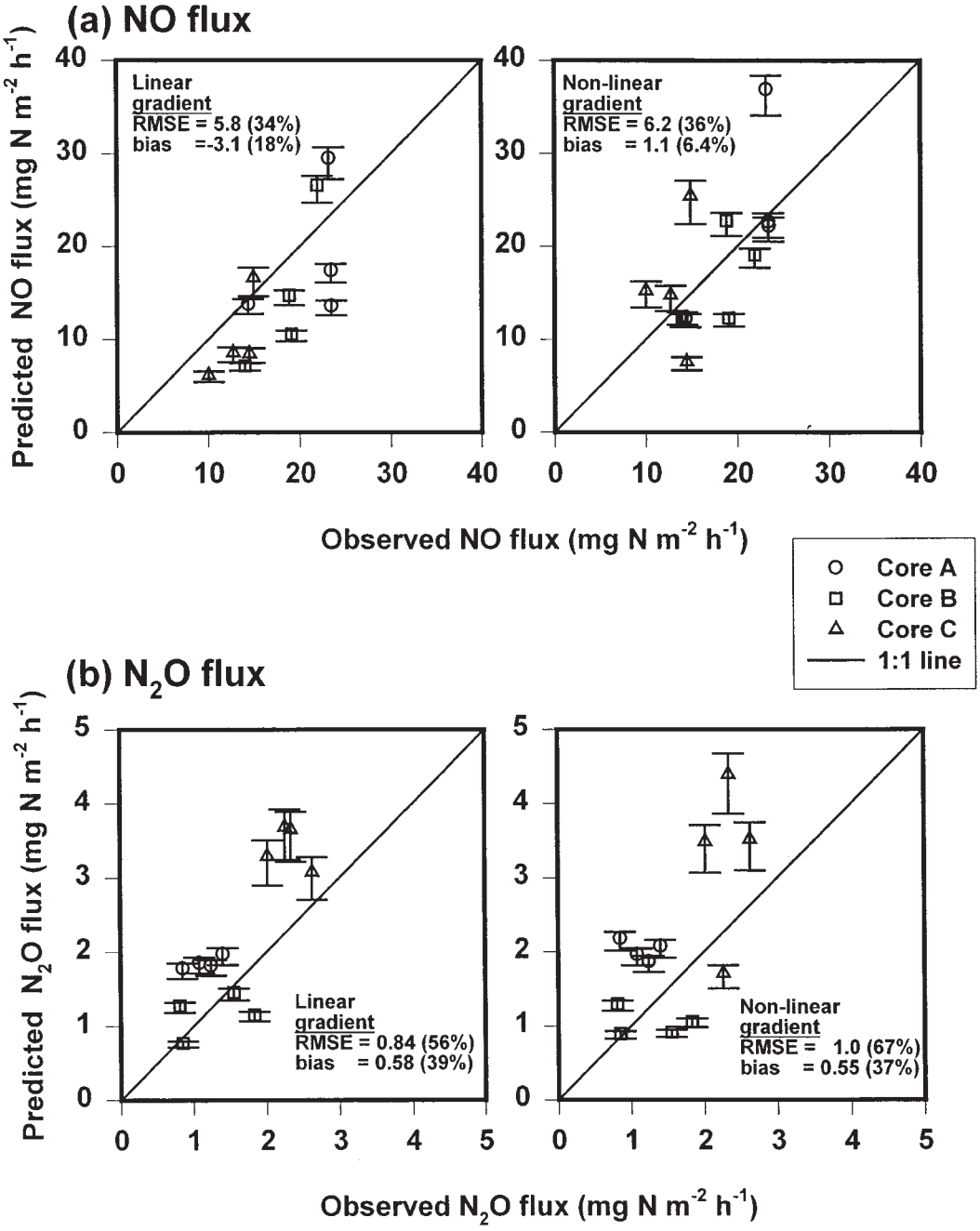

Fig. 6. Fluxes of (a) NO and (b) N_2O from intact cores compared with fluxes predicted using Eqs. (5) and (6) with linear and nonlinear estimates of concentration gradient. Symbols are using Campbell soil-water retention parameter (b) = 5.6. Lower and upper limits of error bars are using b = 3.6 and b = 7.6, respectively. Root-mean square errors (RMSE) and biases are using b = 5.6 (units = mg N m^{-2} h−1; values in parentheses are percentages of mean observed fluxes).

than variation in the b value accounted for the majority of deviation between observed fluxes and those predicted using Eq. [5–6].

Water Content, O_2 and CO_2

Minimal soil drying occurred during the 25- to 30-day experimental periods, i.e., variation in water content values (θ) measured at each depth were not systematic in time (Fig. 7a). Soil bulk density (ρ) over the entire 0.10-m depth was 1,330 $\pm$ 30 kg m^{-3} in Cores A and B. The water contents, therefore, correspond to water-filled porosity values of 40% of total porosity. The O_2 concentrations were only slightly below ambient (>20%) on all occasions, even at the 100-mm depth (Fig. 7b), and showed little variation between cores or over time. Soil-gas CO_2 levels also showed relatively small variations with time. Because O_2 and CO_2 concentrations were relatively constant in time, a steady-state model was used to estimate rates of CO_2 production and O_2 consumption using data in Fig. 7b. Solutions to the diffusion equation with zero-order production (CO_2) or consumption (O_2) with boundary conditions appropriate to the experimental design take the form (Jury, et al., 1991)

$$C_i(z) = \pm \frac{V_i z}{D_{s,i}} \left(L - \frac{z}{2} \right) + C_{o,i} \qquad (7)$$

where C_i is the concentration of species *i* (mmoles CO_2 or O_2 m^{-3} gas), as a function of soil depth (z, m), the ambient concentration ($C_{o,i}$, mmoles CO_2, or O_2 m^{-3} gas) and the reaction parameter (V_i, mmole m^{-3} gas h^{-1}), where V_i is the subsurface respiration ($V_{CO_2} > 0$) or uptake rate ($V_{O_2} < 0$). Average θ and ρ values for each core were used to estimate D_{si} using Eq. (6). Nonlinear regression using functions in the form of Eq. (7) were used to estimate V_{CO_2} and V_{O_2} (solutions plotted in Fig. 7b). Respiration rates and O_2 uptake rates showed good agreement between cores (Table 2). Observed CO_2 molar release rates were significantly lower than the O_2 uptakes rates (V_{CO_2}:V_{O_2} ratios of 0.06–0.08), suggesting that significant amounts of C from the aerobically respired organic matter were utilized for microbial cell synthesis (i.e., immobilized). The V_{O_2} values were then used in the simple-structure model of Arah and Vinten (1995) to estimate the fraction of soil volume in an anaerobic state given by

$$\Phi(z) = \exp\left(-\alpha\, r_\psi^{-\alpha}\, V_{O_2}^{-\beta}\, C_{O_2}^{\gamma} [\theta + \chi\, \epsilon]^{\delta} \right) \qquad (8)$$

where Φ is the anaerobic fraction (m^3 anaerobic soil m^{-3} soil), r_ψ is the radius (m) of a typical air-filled pore at moisture tension ψ(m), χ is the ratio of O_2 diffusivity in free air to that in free liquid (10^4). Values of a (1.5×10^{-10}), α(1.26), β(0.60), γ(0.60), and δ (0.85) are regression parameters found by Arah and Vinten (1995) to provide good approximation ($r^2 = 0.998$) to Φ estimated using more complex models across a range of soil textures and moisture contents. This representation of Φ has also been used successfully in a mechanistic model describing denitrification rates and N_2O emissions in intensively fertilized agricultural fields (Riley and Matson, 2000). In the present case, Φ was calculated as a continuous function of soil depth (z) using the functions for θ and C_{O_2} shown in Fig. 7a–b. Values of ψ and r_ψ were calculated from the capillary rise equation (Jury, et al., 1991), the Core C soil-water retention data (which established a single point relationship between θ and ψ), and the Campbell soil-water retention parameter (b = 5.6 was used). It is clear from Figs. 7a and 7c that the anaerobic fraction predicted using Eq. (8) is a highly nonlinear function of θ, decreasing exponentially below θ values of ~0.20, and that the estimated anaerobic fractions were very low, with maximum Φ values on the order of 10^{-14} and 10^{-10} m^3 anaerobic soil m^{-3} soil for Cores A and B, respectively.

DISCUSSION

Accumulations of NO_2^- in the range of 70–300 mg N kg^{-1}, similar to that found here in the intact cores, have been observed in field studies shortly after AA applications (Chalk, et al., 1975), and similar pH dynamics have also been noted in field studies (Eno and Blue, 1954). Compared with the field experiment (Venterea and Rolston, 2000b) conducted in parallel with the current laboratory study, peak NO_2^- levels were very similar (~100–125 mg N kg^{-1}) as were the pH dynamics. While NO_2^- levels persisted in the field experiment throughout the growing season, concentrations were generally <10 mg N kg^{-1} after the first 10 days. The persistence of higher NO_2^- levels in the laboratory cores may have been attributable to the generally higher field soil temperatures inasmuch as HNO_2 decomposition was shown to be highly sensitive to temperature (Venterea and Rolston, 2000b). Field NO fluxes were generally <4 mg N m^{-2} h^{-1}, or <10–30%, of intact core NO fluxes. As discussed by Venterea and Rolston (2000b), field NO fluxes may have been attenuated by lateral and vertical diffusion of NO out of the AA zone

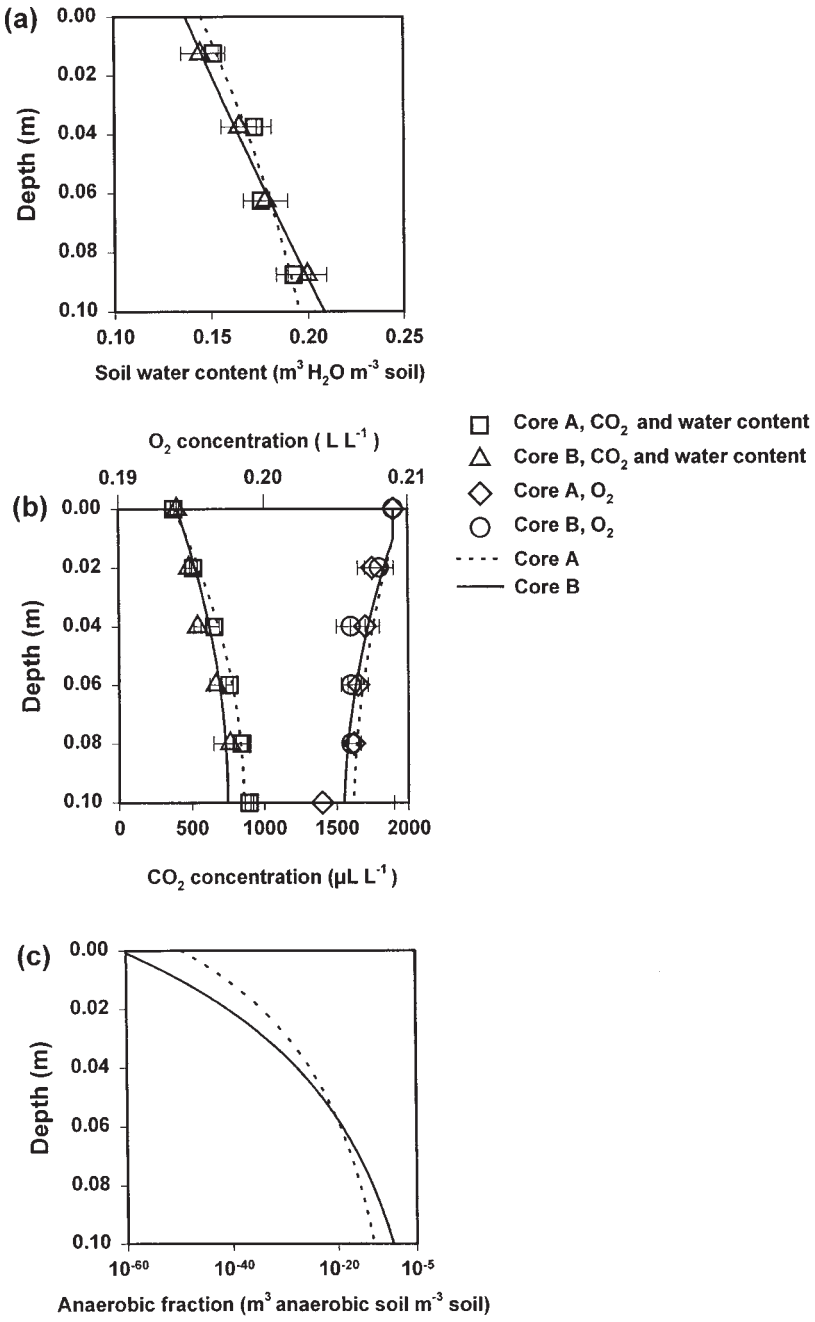

Fig. 7. (a) Soil water contents, (b) soil-gas concentrations of CO_2 and O_2, and (c) estimated anaerobic fractions (Φ). Symbols are mean values (with standard error bars) for all measurements over 25 to 30 days for each core. Lines represent (a) regression functions, (b) solutions to Eq. [7], and (c) calculated Φ values (Eq. [8]).

TABLE 2
Rates of CO_2 respiration and O_2 uptake estimated using Eq. (7)

	mmole CO_2 m^{-3} h^{-1} CO_2 respiration rate V_{CO_2}	mmole O_2 m^{-3} h^{-1} O_2 uptake rate V_{O_2}
Core A	23.6	286
Core B	18.2	303
Mean (SE)†	20.9 (2.7)	295 (8.5)

†SE = standard error (n = 2).

and into unfertilized zones where NO is subject to transformation before reaching the soil surface (Conrad, 1995). Since this process was restricted in the intact core experiments, the pattern of higher NO fluxes in the cores provides further support for this hypothesis. This implies that the very high losses of NO observed from the intact cores (22–37% of the total N initially present, and ~50% of the nitrified N) would not be expected under field conditions. However, this also implies that, in the field, a high fraction (>50%) of the applied N that is nitrified will pass through the NO pool. Therefore, the transport and subsequent fate of NO as it diffuses through the unfertilized zones will be critical in controlling net N losses. These processes may also impact plant availability of N and N leaching losses, depending on the forms of N resulting from NO transformation. Issues related to the transformation of NO are further examined by Venterea and Rolston (2002).

To our knowledge, experimental O_2 and water content concentration profiles have not been used previously to estimate anaerobic fractions at depth within intact soil cores, and simultaneous estimates of anaerobic fractions and soil-gas N_2O concentrations have also not been available. The oxygen uptake rate values (286 − 303 mmole O_2 m^{-3} h^{-1}) obtained using the analysis described here compare well with values obtained using other assumptions (Riley and Matson, 2000). The extremely low anaerobic fractions ($\leq 10^{-10}$) found here, corresponding with high N_2O soil-gas concentrations and surface fluxes, are strong evidence that sources of N_2O other than dissimilatory NO_3^- reduction were important. The highly aerobic conditions also imply that any N_2O produced in the subsurface would likely eventually escape to the atmosphere since (unlike NO) N_2O transformations are mediated exclusively by reductive microbial processes (Firestone and Davidson, 1989). In contrast to NO, field N_2O fluxes were generally higher than the intact core fluxes by a factor of ~5 (Venterea and Rolston, 2000b). The importance of HNO_2 decomposition relative to denitrification as a source of N_2O under the given conditions is evaluated using a diffusion-reaction modeling analysis in Venterea and Rolston (2002).

Some deviation between predicted and observed fluxes (Fig. 6) was expected for several reasons. Soil-gas concentrations were measured at a single point (center of the core), whereas the measured fluxes represent the result of diffusive gradients integrated over the entire soil surface. These gradients could vary significantly as a result of variations in soil physical structure in the upper 5 mm as well as variations in biogeochemical processes driving gas production or consumption. In addition, physical irregularities at the soil surface could cause deviations from the idealized representation of diffusion given by Eq. (5), which assumes one-dimensional diffusion across a perfectly horizontal and uniformly porous boundary. While we attempted to account for this, in part, by measuring soil physical properties close to the boundary, it was not possible to account fully for natural irregularities. Also, while the sweep gas did not create measurable pressure gradients at depths within the core, it is known that a gas stream moving across the boundary of a soil surface can create advective currents within the soil very near to the boundary ($z \leq 5$ mm) (Farrell, et al., 1966). This effect, and all of the effects described above, would also be expected, to some extent, under field conditions. That no consistent pattern of over- or under-estimation was found suggests that no systematic source of transport other than diffusion was important. The teflon rods inserted after each subcore sampling were apparently effective in excluding gas transport and not creating increased edge effects, i.e., there is no pattern of increasing deviation following additional soil samplings for each core. In similar experiments examining NO soil-gas concentrations and surface fluxes in laboratory cores containing sieved and repacked A-horizon forest soil, Rudolph, et al. (1996) concluded that processes other than gaseous diffusion accounted for systematic increases in subsurface gas transport of more than 50% that expected as a result of diffusion. Although a few data points in the present case achieved this degree of deviation (Fig. 6), the lack of a systematic deviation here may have been caused by several factors, including the higher soil bulk density, the use of an improved soil-gas diffusivity model, more precise characterization of physical properties at the soil-atmosphere inter-

face, and experimental verification of minimal subsurface pressure disturbances under dynamic conditions.

CONCLUSIONS

The intact core method was found to be useful in collecting highly resolved subsurface data together with dynamic surface flux measurements of NO and N_2O under isothermal, hydrostatic, and diffusion-dominated conditions. Calculation of system N mass balances, nitrification rates, and integrated gas fluxes revealed that high fractions of the N mass initially present, and of the N undergoing nitrification, were lost primarily as NO at the surface, with smaller losses of N_2O. The chemical and physical conditions suggest that the loss process was driven by nitrification, which caused (a) the accumulation of NO_2^-, and (b) continued reduction in soil pH. These two factors would be expected to generate HNO_2, which is known to decompose abiotically to form NO and N_2O. Comparisons with field flux data suggest that the subsequent transformation of NO as it diffuses to the soil surface will exert significant control over field emissions. This type of controlled study does not necessarily capture the full complexity of field conditions. However, it does allow for detailed process study in cores containing distributions of substrate, water, and physical structure representative of field conditions. The data obtained here also allow for comparisons to mechanistic transport and transformation models, as described in the companion paper (Venterea and Rolston, 2002).

ACKNOWLEDGMENTS

The authors gratefully acknowledge D. Paige for assistance with design and fabrication of the soil core apparatus and P. Moldrup for helpful discussion. This work was supported in part by the Kearney Foundation of Soil Science, and in part by the U.S. EPA (R819658 & 825433) Center for Ecological Health Research at UC Davis, although it may not necessarily reflect the views of the EPA, and no official endorsement should be inferred.

REFERENCES

Allison, F. 1955. The enigma of soil nitrogen balance sheets. Adv. Agron. 7:213–250.

Arah, J. R. M., and A. J. A. Vinten. 1995. Simplified models of anoxia and denitrification in aggregated and simple-structure soils. Eur. J. Soil Sci. 46:507–517.

Bird, R., W. Stewart, and E. Lightfoot. 1960. Transport Phenomena. John Wiley & Sons, New York.

Bouman, O., D. Curtin, C. Campbell, V. Biederbeck, and H. Ukrainetz. 1995. Soil acidification from long-term use of anhydrous ammonia and urea. Soil Sci. Soc. Am. J. 59:1488–1494.

California Department of Food and Agriculture. 1998. Fertilizing materials tonnage report. Sacramento, January–June.

Chalk, P., D. Keeney, and L. Walsh. 1975. Crop recovery and nitrification of fall and spring applied anhydrous ammonia. Agron. J. 67: 33–41.

Clapp, R. B., and G. M. Hornberger. 1978. Empirical equations for some soil hydraulic properties. Water Resour. Res. 14:601–604.

Collison, R., H. Beattie, and J. Harlan. 1933. Lysimeter investigations: III. Mineral and water balance in legume and non-legume crop rotations for a period of 16 years. NY (Geneva) Agric. Exp. Sta. Tech. Bull., Cornell University 212:1–81.

Conrad, R. 1995. Metabolism of nitric oxide in soil and soil microorganisms and regulation of flux into the atmosphere. *In* Microbiology of Atmospheric Trace Gases: Sources, Sinks and Global Processes. J. C. Murrell, and D. P. Kelly (eds.). Springer, New York, pp. 167–201.

Crutzen, P. 1981. Atmospheric chemical processes of the oxides of nitrogen, including nitrous oxide. *In* Denitrification, Nitrification and Atmospheric N_2O. C. Delwiche (ed.). John Wiley & Sons, Chichester, UK, pp. 17–44.

Curtin, D., C. Campbell, and A. Jalil. 1998. Effects of acidity on mineralization: pH-dependence of organic matter mineralization in weakly acidic soils. Soil Biol. Biochem. 30:57–64.

Eno, C., and W. Blue. 1954. The effect of anhydrous ammonia on nitrification and the microbiological population in sandy soils. Soil Sci. Soc. Am. Proc. 18:178–181.

Farrell, D., E. Greacen, and C. Gurr. 1966. Vapor transfer in soil due to air turbulence. Soil Sci. 102:305–313.

Firestone, M., and E. Davidson. 1989. Microbiological basis of NO and N_2O production and consumption in soil. *In* Exchange of Trace Gases between Terrestrial Ecosystems and the Atmosphere. M. Andreae, and D. Schimel (eds.). John Wiley & Sons, Chichester, UK, pp. 7–21.

Hutchinson, G., and E. Davidson. 1993. Processes for production and consumption of gaseous nitrogen oxides in soil. *In* Agricultural Ecosystem Effects on Trace Gases and Global Climate Change, ASA Special Publication no. 55. D. Rolston, L. Harper, A. Mosier, and J. Duxbury (eds). Am. Soc. Agron., Crop Sci. Soc. Am. , and Soil Sci. Soc. Am., Madison, WI, pp. 79–83.

Jury, W., W. Gardner, and W. Gardner. 1991. Soil Physics. John Wiley & Sons, New York.

Kroeze, C., A. Mosier, and L. Bouwman. 1999. Closing the global N_2O budget: A retrospective analysis 1500 – 1994. Global Biogeochem. Cycles. 13:1–8.

Matson, P., C. Billow, and S. Hall. 1996. Fertilization

practices and soil variations control nitrogen oxide emissions from tropical sugar cane. J. Geophys. Res.- Atmos. 101(D13):18.,533–18,545.

Moldrup, P., C. Kruse, D. Rolston, and T. Yamaguchi. 1996. Modeling diffusion and reaction in soils: III. Predicting gas diffusivity from the Campbell soil-water retention model. Soil Sci. 161:366–375.

Moldrup, P., T. Olesen, D. Rolston, and T. Yamaguchi. 1997. Modeling diffusion and reaction in soils: VII. Predicting gas and ion diffusivity in undisturbed and sieved soils. Soil Sci. 162:632–640.

Moldrup, P., T. Olesen, T. Yamaguchi, P. Schjonning, and D. Rolston. 1999. Modeling diffusion and reaction in soils: IX. The Buckingham-Burdine-Campbell equation for gas diffusivity in undisturbed soil. Soil Sci. 164:542–551.

Moraghan, J. 1980. Precautions on the use of anhydrous ammonia applicators in research plots. Agron. J. 72:157–160.

Riley, W., and P. Matson. 2000. NLOSS: A mechanistic model of denitrified N_2O and N_2 evolution from soil. Soil Sci. 165:237–249.

Rolston, D., and P. Moldrup. 2002. Gas diffusivity. *In* Methods of Soil Analysis, Part 1, Physical Methods, 3rd Ed. G.C. Topp and J.H. Dane (eds.). Soil Sci. Soc. Am., Madison, WI (*in press*).

Röver, M., O. Heinemyer, and E. Kaiser. 1998. Microbial induced nitrous oxide emissions from an arable soil during winter. Soil Biol. Biochem. 30:1859–1865.

Rudolph, J., F. Rothfuss, and R. Conrad. 1996. Flux between soil and atmosphere, vertical concentration profiles in soil, and turnover of nitric oxide: 1. Measurements on a model soil core. J. Atmos. Chem. 23:253–273.

Soil Conservation Service. 1993. Soil Survey of Sacramento County, California. United States Department of Agriculture.

Stehouwer, R., and J. Johnson. 1990. Urea and anhydrous ammonia management for conventional tillage corn production. J. Prod. Agric. 3:507–513.

Strong, W., and J. Cooper. 1992. Application of anhydrous ammonia or urea during the fallow period for winter cereals on the Darling Downs, Queensland. Aust. J. Soil Sci. 30:695–709.

Thornton, F. C., and R. J. Valente. 1996. Soil emissions of nitric oxide and nitrous oxide from no-till corn. Soil Sci. Soc. Am. J. 60:1127–1133.

Van Cleemput, O., and A. Samater. 1996. Nitrite in soils: Accumulation and role in the formation of gaseous N compounds. Fert. Res. 45:81–89.

Venterea, R., and D. Rolston. 2000a. Mechanisms and kinetics of nitric and nitrous oxide production during nitrification in agricultural soil. Global Change Biol. 6:1–14.

Venterea, R., and D. Rolston. 2000b. Nitric and nitrous oxide emissions following fertilizer application to agricultural soil: Biotic and abiotic mechanisms and kinetics. J. Geophys. Res.-Atmos. 105(D12):15., 117–15,129.

Venterea, R., and D. Rolston. 2002. Nitrogen oxide trace gas transport and transformation: II. Model simulations compared to data. Soil Sci. 167:49–61.

Vitousek, P. M., and P. A. Matson. 1993. Agriculture, the global nitrogen cycle, and trace gas flux. *In* Biogeochemistry of Global Change: Radiatively Active Trace Gases. R. S. Oremland (ed.). Chapman & Hall, New York, pp. 193–208.